The Plant Cell, Vol. 14, 547–558, March 2002, www.plantcell.org © 2002 American Society of Plant Biologists

RESEARCH ARTICLE

# *KNAT1* and *ERECTA* Regulate Inflorescence Architecture in Arabidopsis

**Scott J. Douglas,[a] George Chuck,[b] Ronald E. Dengler,[a] Lakshmi Pelecanda,[a] and C. Daniel Riggs[a,1]**

[a] Botany Department, University of Toronto, 1265 Military Trail, West Hill, Ontario M1C1A4, Canada
[b] Biology Department, University of California, San Diego, 9500 Gilman Drive, La Jolla, California 92093-0116

**Plant architecture is dictated by morphogenetic factors that specify the number and symmetry of lateral organs as well as their positions relative to the primary axis. Mutants defective in the patterning of leaves and floral organs have provided new insights on the signaling pathways involved, but there is comparatively little information regarding aspects of the patterning of stems, which play a dominant role in architecture. To this end, we have characterized five alleles of the *brevipedicellus* mutant of Arabidopsis, which exhibits reduced internode and pedicel lengths, bends at nodes, and downward-oriented flowers and siliques. Bends in stems correlate with a loss of chlorenchyma tissue at the node adjacent to lateral organs and in the abaxial regions of pedicels. A stripe of achlorophyllous tissue extends basipetally from each node and is positioned over the vasculature that services the corresponding lateral organ. Map-based cloning and complementation studies revealed that a null mutation in the *KNAT1* homeobox gene is responsible for these pleiotropic phenotypes. Our observation that wild-type Arabidopsis plants also downregulate chlorenchyma development adjacent to lateral organs leads us to propose that KNAT1 and ERECTA are required to restrict the action of an asymmetrically localized, vasculature-associated chlorenchyma repressor at the nodes. Our data indicate that it is feasible to alter the architecture of ornamental and crop plants by manipulating these genetically defined pathways.**

## INTRODUCTION

The generation of asymmetries is an underlying theme in the development of higher eukaryotes. Organismal complexity arises progressively through the deposition and interpretation of positional information that refines and elaborates previously established spatial and temporal patterns. In plants, shoot and inflorescence development can be visualized as a reiterative process generating successively greater numbers of leaves, axillary meristems, and stems. The establishment and maintenance of this pattern requires the action of molecular switches that respond to positional information and mediate sharp transitions between different types of tissue and cellular identities. Loss of patterning factors in mutants can result in the transformation of cellular and tissue identities of one region to those characteristic of other locations, thus producing morphological novelties (Bowman, 2000; Ng and Yanofsky, 2001).

In higher plants, the formation of aerial organs is dependent on the activity of the shoot apical meristem (SAM), a dome-shaped morphogenetic field in which organ primordia are initiated. The SAM is divided into a central zone of undifferentiated initial cells, a peripheral zone in which lateral organs are initiated, and a basal rib zone in which stem tissue is specified. The SAM thus exhibits radial and apical-basal polarity as well as heterogeneity around its circumference. These asymmetries are necessary for proper SAM functioning and continued organ initiation throughout the life of the plant, but they also may contribute more directly to organ development by regulating patterns of shoot morphogenesis and differentiation. For example, during vegetative development, leaves are initiated at the peripheral zone of the SAM and undergo morphogenesis and differentiation so that, in most species, the adaxial (dorsal) and abaxial (ventral) sides of the leaf adopt distinct features (for review, see Bowman, 2000). Recently, a link between the radial (inside-outside) organization of the shoot and dorsoventral leaf patterning was established, suggesting that patterns of leaf morphogenesis may depend on the perception and interpretation of shoot-associated radial asymmetries (Kerstetter et al., 2001; McConnell et al., 2001). These findings present the SAM as an active organizer that functions during organogenesis to project asymmetries onto early primordia and direct spatially distinct developmental programs.

Superimposed on the radial pattern of shoots are variations in tissue characteristics around the SAM's circumference,

[1] To whom correspondence should be addressed. E-mail riggs@utsc.utoronto.ca; fax 416-287-7642.
Article, publication date, and citation information can be found at www.plantcell.org/cgi/doi/10.1105/tpc.010391.

which are reflected in the incorporation of subsets of peripheral zone cells into organ primordia. Most commonly, primordia are initiated in succession at the SAM so that mature organs are arranged around the stem in a spiral phyllotaxy. In many upright plants, lateral organ elaboration is accompanied by the elongation of stem tissue to form internodes that punctuate stem–lateral organ junctions (nodes) along the vertical axis. In contrast to the nodes, which in plants with a spiral phyllotaxy exhibit obvious circumferential asymmetries, internodes appear radialized. It is not known how the heterogeneous circumferential pattern of the SAM is altered to produce seemingly radialized internodes.

Studies of the genetic control of stem development have focused on internode elongation. Arabidopsis mutants with reduced internode lengths include *erecta* (*er*), *acaulis*, *brevipedicellus* (*bp*), and gibberellic acid auxotrophs (Koornneef et al., 1983; Tsukaya et al., 1993; Torii et al., 1996; Hanzawa et al., 1997; McCourt, 1999). In the case of *er* and *bp*, the pedicels, which are specialized internodes that support and orient flowers and fruit at an upward angle on the inflorescence stem, also are reduced in length. *bp* stems also bend during development, resulting in an altered architecture characterized by downward-oriented pedicels and bends in the inflorescence stem at nodes. Although the molecular characterization of the *BP* gene has not been reported, *ER* encodes a receptor protein kinase that is expressed in the SAM and organ primordia, implicating intercellular signaling networks in the regulation of stem development (Torii et al., 1996; Yokoyama et al., 1998).

In rice, a number of mutants have been characterized and grouped on the basis of the elongation pattern of the upper four or five internodes. One of these mutants exhibited shortened internodes and altered patterns of epidermal and subepidermal cell differentiation as a result of a loss-of-function mutation in the *OSH15 KNOTTED*-like homeobox (*KNOX*) gene (Sato et al., 1999). *KNOX* genes encode putative transcription factors that have been divided into two classes on the basis of sequence similarities and expression domains (Kerstetter et al., 1994). Class I genes, which include *OSH15*, are expressed predominantly in meristematic tissues and generally are downregulated as cells are recruited into organ primordia (Reiser et al., 2000). In contrast, class II genes are expressed in differentiating organs such as leaves, flowers, and roots. Because of variations in the expression patterns and the paucity of mutants in different class II genes, their roles have not been investigated thoroughly.

Through loss- and gain-of-function studies, class I *KNOX* genes have been implicated as regulators of meristem function in both monocots and dicots (Reiser et al., 2000). Recessive mutations in the Arabidopsis *KNOX* gene *SHOOT MERISTEMLESS* (*STM*) give rise to plants that do not form a functional SAM (Barton and Poethig, 1993; Long et al., 1996), whereas shoot development terminates prematurely in maize plants lacking *KNOTTED1* function (Vollbrecht et al., 2000). Ectopic expression of class I *KNOX* genes in maize leaves results in the localized overproliferation of adaxial leaf cells and the conversion of distal leaf tissue to fates associated with cells found closer to the base of the leaf (Sinha et al., 1993; Schneeberger et al., 1995; Muehlbauer et al., 1999). In addition, a number of *KNOX* genes from Arabidopsis, rice, tobacco, and maize are sufficient to induce the ectopic formation of SAMs on adaxial leaf surfaces when overexpressed in certain plant species (Chuck et al., 1996; Williams-Carrier et al., 1997; Nishimura et al., 2000; Sentoku et al., 2000). These and other studies implicate class I *KNOX* genes in the establishment and maintenance of meristems, possibly serving in a switch mechanism that governs indeterminate to determinate development.

We are interested in the molecular mechanisms that dictate the architecture of higher plants. We investigated the mechanisms underlying stem morphogenesis by characterizing the *bp* mutant of Arabidopsis. We found that the *bp* phenotype is caused by a loss-of-function mutation in the class I *KNOX* gene *KNAT1*, and we provide evidence that *KNAT1* functions along with *ERECTA* to radialize internodes and pedicels during stem elongation.

## RESULTS

### The *BP* Gene Promotes Cell Division and Elongation in Internodes

During Arabidopsis vegetative development, leaves are formed in the absence of internode elongation, resulting in a rosette. The perception of floral inductive cues represses leaf development, initiates floral primordia outgrowth at the SAM, and induces elongation of stem tissue to form internodes. During floral morphogenesis, the determinate floral meristem gives rise to a conserved number and pattern of organs, whereas the basal portion of the primordium elongates to form the pedicel, the short stalk connecting the flower to the inflorescence stem. We have examined five independent alleles of the developmental form mutant *bp*. The original ethyl methanesulfonate–induced *bp* mutant (Koornneef et al., 1983) we have termed *bp-1*, and additional alleles were termed *bp-2* through *bp-5*. In *bp* mutants, both internodes and pedicels are reduced in length and stem tissue develops bends that significantly alter shoot architecture. Pedicels bend downward so that the orientation of flowers and siliques is reversed relative to the wild type, and bends develop in inflorescence stems at leaf and floral nodes (Figure 1, Table 1). In the inflorescence stem, lateral organs always are elaborated on the concave side of the bend, and stripes of achlorophyllous tissue, initiated below the nodes, spiral down the stem (Figures 1C and 1D).

Morphometric analyses revealed that *bp* plants are significantly shorter than wild-type (Landsberg *erecta* [L*er*]) plants, which could be attributable to a defect in internodal

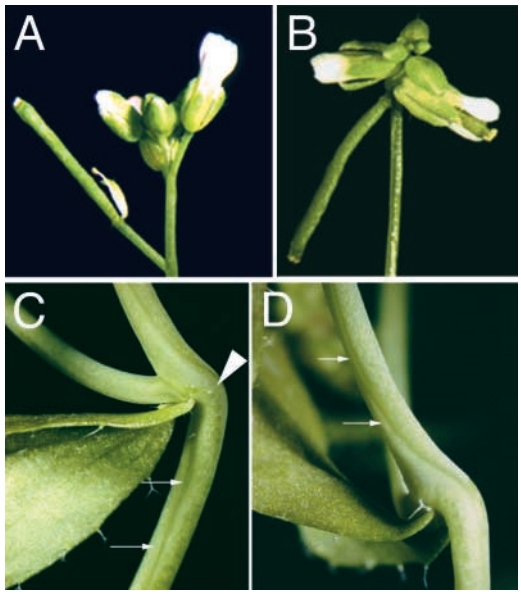


**Figure 1.** Inflorescence Phenotypes of L*er* and *bp-2* Plants.

**(A)** Wild-type L*er* inflorescence exhibiting upright flowers and a long pedicel.
**(B)** *bp-2* inflorescence exhibiting downward-pointing flowers and siliques and very short pedicels.
**(C)** and **(D)** *bp-2* plants exhibiting bends at nodes (arrowhead) and stripes of achlorophyllous tissue (arrows).

cell division, cell elongation, or both. To distinguish between these possibilities, we compared the epidermal cell lengths of *bp* internodes with those of L*er*. We observed that L*er* cells have an average length of 291 μm, whereas *bp* cells average 249 μm, or 86% of the wild-type length (data not shown). Taking into account the morphometric data (Table 1), it is apparent that there is both a cell expansion defect and a cell division defect in the mutant. However, not all cells are affected. Cells of the elongating stems and pedicels are most susceptible, whereas there are no obvious differences in leaf shape or size or in floral organ size or morphology.

**Table 1.** Influence of *BP* and *ER* Alleles on Plant Architecture

| Genotype | Height (cm) | Pedicel Length (cm) | Pedicel Angle (°) |
|---|---|---|---|
| *BP/ER* | 22.5 ± 0.3 | 0.87 ± 0.01 | 60 ± 1 |
| *BP/er* | 11.3 ± 0.3 | 0.37 ± 0.01 | 55 ± 2 |
| *bp/ER* | 17.1 ± 0.4 | 0.42 ± 0.06 | 106 ± 3 |
| *bp/er* | 5.2 ± 0.1 | <0.1 | 143 ± 2 |

Plants ($n \geq 16$) were measured 39 days after germination. Values given are averages ±SEM.

## Chlorenchyma Density Is Reduced Adjacent to Wild-Type Lateral Organs

To gain an understanding of the processes disrupted during *bp* stem morphogenesis, we examined wild-type and mutant stem anatomies. Because the *ERECTA* gene is known to influence stem morphogenesis and plant architecture, and because our *bp* mutants were generated in a L*er* genetic background, we first characterized wild-type Landsberg (Lan; see Methods) plants to obtain a baseline for internode, node, and pedicel anatomies. Transverse sections through Lan internodes and pedicels revealed a stereotypical radial pattern consisting of a single layer of epidermis, four to five layers of ground tissue (chlorenchyma), a layer of alternating vascular bundles and interfascicular fibers, and a central pith (Figure 2A). The relatively uniform distribution of chloroplasts in the cortex of pedicels and internodes, and of stomata in the epidermal layers, gives these tissues a radialized appearance, although internodes and pedicels as a whole are radially asymmetric as a result of vascular bundle spacing and size heterogeneity. Variations in vascular bundle size are particularly evident at the base of Lan pedicels, where adaxial bundles are much smaller (Figure 2A).

In contrast to internodes and pedicels, all tissues are radially asymmetric at Lan nodes because of anatomical changes associated with the branching of lateral organs (Figure 2B). Most obvious is the absence of a discrete vascular bundle in the stem adjacent to the region of attachment of the lateral organ. This gap is formed as a result of the subnodal branching of a main stem bundle into the lateral organ to facilitate the exchange of water, metabolites, and signaling molecules between the organ and the rest of the plant. We also have found that the continuous distribution of chlorenchyma tissue in cortical regions of the internode is interrupted adjacent to lateral organs at the nodes, producing a collar of achlorophyllous tissue (Figure 2B). This perturbation in chloroplast density extends longitudinally to the top of the node, where a gap in the chlorenchyma distribution is apparent directly above the lateral organs (Figure 2C). The achlorophyllous cortex extends <100 μm above the node, past which the internode assumes its characteristic chlorenchyma radial pattern. These data indicate that the downregulation of chlorenchyma development occurs adjacent to lateral organs in wild-type Arabidopsis plants.

The *ERECTA* gene influences multiple processes during Arabidopsis development, including internode and pedicel elongation and leaf and silique morphogenesis. Stem tissue thickness is increased in L*er* plants, resulting in a more erect, rigid appearance. In general, we have found that increases in L*er* stem thickness correlate with the enhanced development of supporting schlerenchyma tissue in internodes and pedicels (Figures 2D and 2E). Hand sections

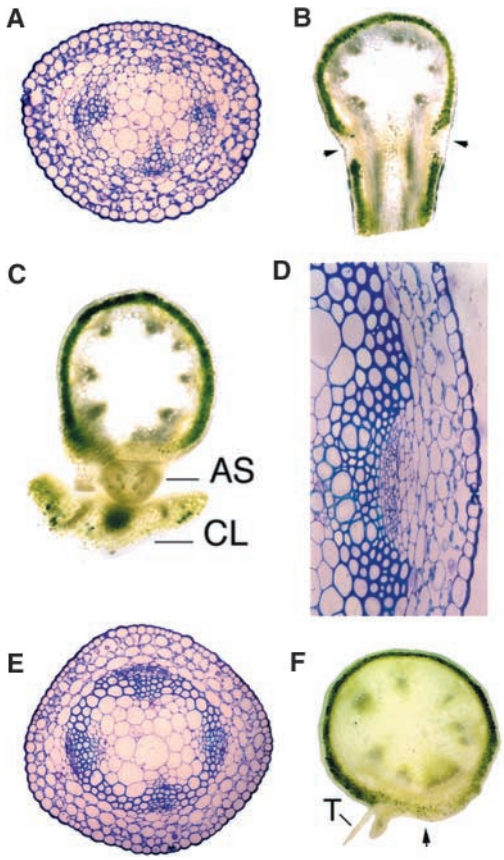


**Figure 2.** Anatomy of Lan and L*er* Stems.

**(A)** Toluidine blue–stained cross-section of the proximal end of a Lan pedicel. The abaxial side is oriented toward the bottom.
**(B)** Hand section through a Lan floral node showing radial asymmetry. Arrowheads point to regions in which chlorenchyma development is repressed.
**(C)** Hand section above a Lan vegetative node illustrating a gap in chlorenchyma tissue directly above the lateral organ. AS, axillary stem; CL, cauline leaf.
**(D)** Toluidine blue–stained cross-section of a L*er* internode. Note that cortical cells contain numerous chloroplasts and that supporting sclerenchyma tissue is abundant.
**(E)** Toluidine blue–stained cross-section at the proximal end of a L*er* pedicel with the abaxial side oriented toward the bottom.
**(F)** Hand section through the base of a L*er* vegetative node showing that the region of achlorophyllous tissue includes stem regions at the base of lateral organs. The leaf base is indicated by the arrow. T, trichome.

through L*er* nodes also have revealed that the chlorenchyma downregulation observed adjacent to and above Lan lateral organs is expanded in L*er* to include stem regions at the bases of leaves and flowers, implicating a role for *ER* in regulating chlorenchyma tissue development (Figure 2F).

### *bp* Internodes Form Chlorenchyma-Deficient Stripes That Extend Basipetally from Nodes

We next examined node, internode, and pedicel anatomies of *bp-2* plants using light and scanning electron microscopy. Analyses of *bp-1*, *bp-3*, and *bp-4* yielded similar results, but *bp-5* defects were less severe as a result of the presence of a wild-type *ER* gene (see below). We found that the asymmetric distribution of chlorenchyma tissue observed directly above the lateral organs in Lan and L*er* is expanded to include a larger portion of the stem circumference in *bp* (Figure 3A). Furthermore, although achlorophyllous cortex is confined to nodal regions in L*er* and Lan, regions of reduced chlorenchyma density extend basipetally from cauline leaf and floral nodes into underlying internodes in *bp* (Figure 3B). These stripes of achlorophyllous tissue always initiate directly beneath lateral organs, suggesting that they are related to the asymmetric chlorenchyma distribution observed adjacent to wild-type lateral organs. Achlorophyllous cortical tissue also was observed on the abaxial and lateral sides of *bp* pedicels (Figure 3C). Toluidine blue–stained transverse sections through *bp* internodes and pedicels demonstrate that the downregulation of chlorenchyma tissue correlates with a loss of stomata in the epidermis and a reduction in intercellular spaces in subepidermal layers (Figures 3D and 3E). These characteristics also are evident in epidermal and subepidermal whole mounts (Figures 3F and 3G).

In the epidermis, loss of stomata results in the alignment of epidermal cells into discrete files, which can be visualized using scanning electron microscopy on internode and pedicel surfaces (Figures 3H and 3I). In contrast, the abaxial side of L*er* pedicels shows no evidence of a stripe (Figure 3J). Scanning electron microscopy confirmed that stripes initiate below the lateral organs along the inflorescence stem and extend proximodistally on the abaxial side of the pedicel. Occasionally, stripes extend beyond a single internode's length, resulting in two or more stripes on the same internode (Figures 1C, 1D, and 3B). Therefore, our microscopy data link anatomical defects with the morphological abnormalities that characterize *bp*. Specifically, *bp* internodes and pedicels lack cortical and epidermal radial symmetry on the abaxial region of pedicels and in internodes below the lateral organs. Furthermore, the similarity between the stripes of achlorophyllous tissue in *bp* internodes and pedicels and the wild-type nodal chlorenchyma distribution suggests that *bp* anatomical abnormalities may be patterned through the action of mechanisms at work during normal nodal development.

### *bp* Stripes Are Associated with the Vasculature

In our analysis of *bp* internode anatomy, we observed that each stripe of achlorophyllous tissue was always positioned over a vascular bundle. To determine whether the position of

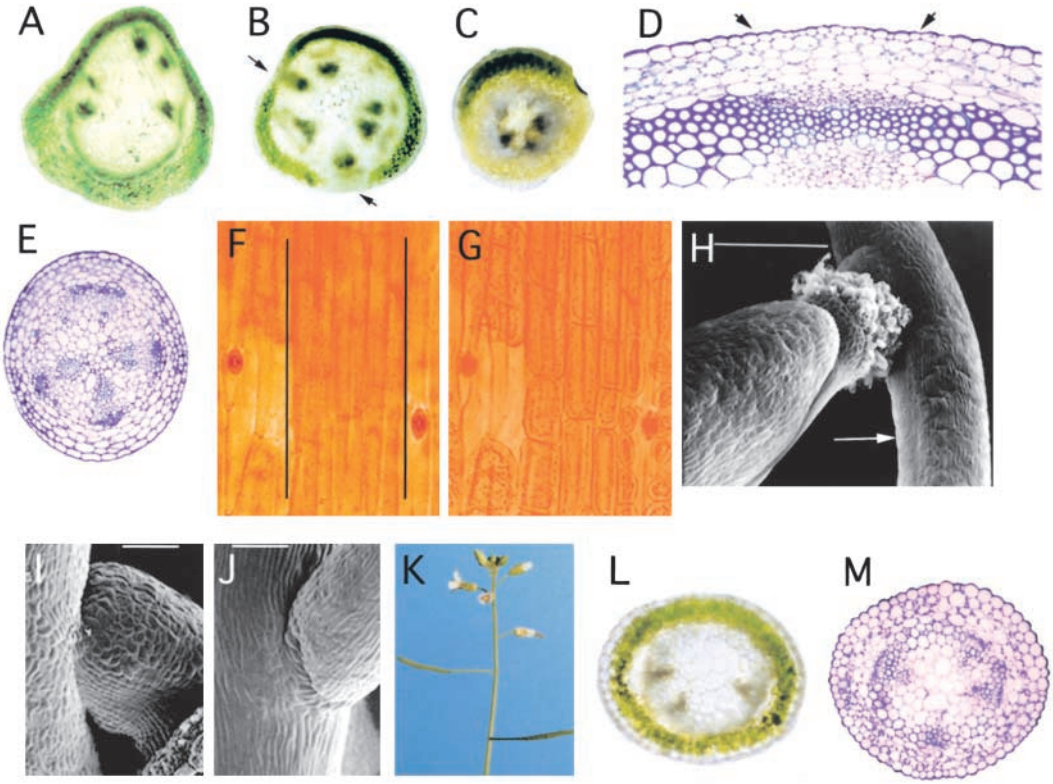


**Figure 3.** Morphological Analysis of *bp-2*.

**(A)** Hand section above a vegetative node. Note that the region of achlorophyllous tissue is expanded relative to Lan (cf. with Figure 2C).
**(B)** Hand section through an internode. Arrows indicate reductions in cortical chlorenchyma over two vascular bundles.
**(C)** Hand section through a pedicel with the abaxial region at the bottom.
**(D)** Toluidine blue–stained cross-section of an internode. The stripe region is defined by the arrows (cf. with Figure 2D). The epidermal cells are narrower, and chloroplast density is reduced in all cortical cell layers. Note that the stripe occurs over a vascular bundle.
**(E)** Toluidine blue–stained pedicel cross-section. The abaxial region is located at the bottom, and chloroplasts and intercellular spaces are scarce (cf. with Figure 2E).
**(F)** Safranin-stained stem epidermis showing a stripe that is devoid of stomata surrounded by nonstripe regions containing stomata. Black horizontal lines delimit the region of the stripe.
**(G)** Subepidermal (L2) layer of **(F)**. Note the large block-like cells underlying the stripe and the lack of intercellular space. In contrast, the shadows of stomata can be seen in the nonstripe areas, cells in this area are smaller and rounder, and considerable intercellular space exists.
**(H)** Scanning electron micrograph of a *bp* stem illustrating the files of cells that constitute the stripe (arrow).
**(I)** Scanning electron micrograph of a *bp* pedicel/stem junction showing files of cells on the pedicel abaxial surface.
**(J)** Pedicel/stem junction of a L*er* plant showing the abaxial surface of the pedicel.
**(K)** *bp*/*ER* plant showing that a wild-type *ER* gene suppresses the severity of the pedicel angle.
**(L)** Hand section through a *bp*/*ER* pedicel showing continuous distribution of mature chlorenchyma (cf. with Figure 3C) tissue. The abaxial side is oriented toward the bottom.
**(M)** Toluidine blue–stained cross-section of a *bp*/*ER* pedicel.
Bar in **(H)** = 400 μm; bars in **(I)** and **(J)** = 100 μm.

the stripe in *bp* internodes is linked to the vasculature associated with particular lateral organs, we made a series of hand sections through the *bp* stem at the node and in the underlying internode (Figure 4A). We found that as stripes extend down an internode, they always are positioned over the same vascular bundle and that the stripes and the vascular bundles they overlie are associated with the same lateral organs. This result is consistent with the notion that the stripes of achlorophyllous tissue observed in *bp* internodes are extensions of wild-type nodal asymmetries and that the *BP* gene is required for the activation of chlorenchyma development during internode elongation. Hand sections through internodes of L*er*

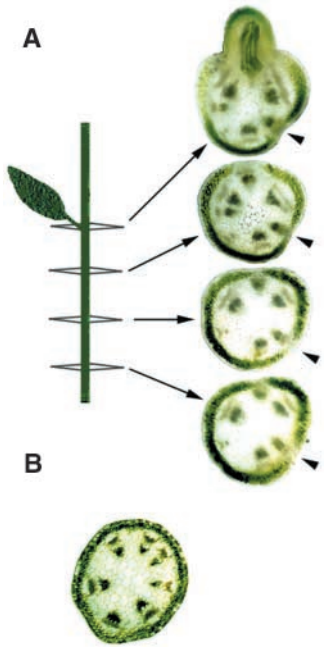


**Figure 4.** Stripes Are Associated with Specific Underlying Vascular Bundles.

**(A)** Left, diagram of a stem showing a node with its associated lateral organ. Right, hand sections of a *bp* stem corresponding to regions shown in the diagram. The top section is oriented with the stripe-associated lateral organ at the top. Subsequent sections are oriented similarly, which can be confirmed by observing the arrangement of vascular bundles. The position of a second stripe, initiated from a superior node, is marked by arrowheads.
**(B)** Hand section through an internode of a L*er* plant illustrating a continuous ring of chlorenchyma tissue.

(Figure 4B) and Lan (data not shown) showed no evidence of discontinuities in chlorenchyma patterning.

### A Functional *ERECTA* Gene Suppresses the *bp* Phenotype

Because the *bp* mutation is in an *erecta* background and the *ERECTA* gene influences stem elongation and nodal chlorenchyma patterning, we crossed *bp* with Lan to observe the single mutant *bp/ER* phenotype. These plants were shorter than Lan plants, pedicels were reduced in length, and siliques were oriented approximately perpendicular to the inflorescence axis (Figure 3K, Table 1). In addition, more subtle bends were observed in the inflorescence stem at the nodes. Although sections through *bp/ER* pedicels revealed achlorophyllous abaxial and lateral regions, no stripe was evident in *bp/ER* pedicels (Figures 3L and 3M). In the inflorescence stem, a stripe was present in *bp/ER* internodes beneath lateral organs, but it did not extend as far down the stem as in *bp* plants (data not shown). These results indicate that the *BP* and *ER* genes have overlapping roles in regulating plant architecture and chlorenchyma differentiation in stem tissue.

In summary, *bp* morphological defects correlate with abnormal patterns of tissue differentiation in internodes and pedicels. The similarity of chlorenchyma patterning in *bp* internodes and pedicels to wild-type nodal asymmetries, combined with the association of vasculature and stripes with common lateral organs, suggests that altered internode and pedicel patterns of differentiation in *bp* may be extensions of wild-type nodal characteristics. Furthermore, these results demonstrate that the *ER* gene functions redundantly with *BP* to influence plant architecture and stem differentiation.

### The *bp* (L*er*) Phenotype Is Caused by a Mutation in the Class 1 Homeobox Gene *KNAT1*

We used a map-based cloning strategy to clone the gene responsible for the *bp* mutant phenotype (Figure 5A). Because *bp* is used as a visible marker for chromosome 4, we focused on the segregation of molecular markers near the centromere. By mapping, we were able to focus on a region of ~200 kb, all of which had been sequenced completely by the Arabidopsis Genome Initiative (2000). Two of our mutants (*bp-2* and *bp-3*) were generated by fast neutron bombardment, which often generates large deletions, and we first examined these by polymerase chain reaction and DNA gel blot analysis to determine if these mutants exhibited any differences in DNA content from the wild type. In both of these mutants, large chromosomal segments had been deleted, and interestingly, two of the other three alleles also were caused by deletions (Table 2). The fifth allele, generated by ethyl methanesulfonate, gave rise to wild-type patterns of hybridization (Figure 5B). From Arabidopsis Genome Initiative annotations, one of the most likely candidate genes was the *KNOTTED*-like homeobox gene *KNAT1*. Sequencing of *KNAT1* in *bp-4* revealed an A-to-G transition mutation at the splice donor site of the third exon, which presumably results in missplicing of the mRNA. We transformed *bp-1* and *bp-2* plants with a genomic *KNAT1* fragment and recovered several fully complemented transformants from each allele (data not shown). Collectively, these results demonstrate that the *bp* phenotype is attributable to a loss-of-function mutation in the *KNAT1* gene. To conform to community standards for naming Arabidopsis genes, hereafter we refer to the gene as *BP*.

### *BP* Expression Domains

Previous studies have shown that *BP* is expressed during inflorescence development in internodes, pedicels, and carpels (Lincoln et al., 1994). We have investigated its expression pattern further using in situ hybridization and β-glucuronidase (GUS) staining of transgenic plants harboring a

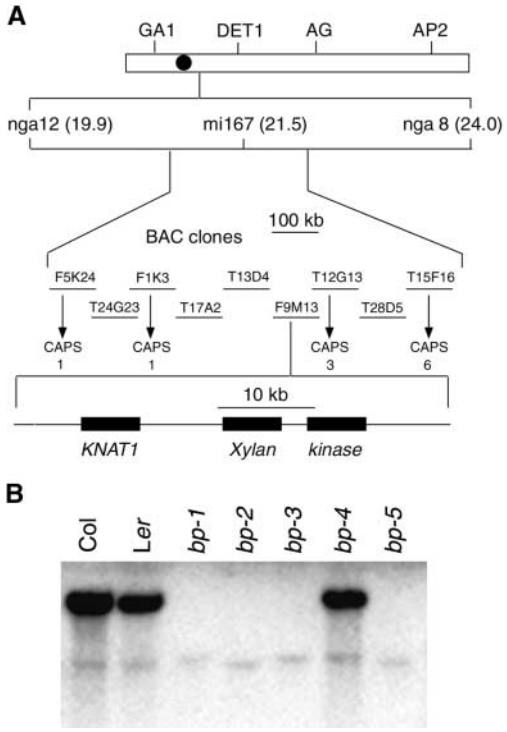


**Figure 5.** Positional Cloning of the *BP* Gene and Molecular Analysis of Five Mutant Alleles.

**(A)** Summary of mapping data and chromosomal location of the *BP* locus. A scheme of chromosome 4 is shown at the top. Simple sequence length polymorphism (nga8, nga12) and restriction fragment length polymorphism (mi167) markers and their respective map positions are shown along with the bacterial artificial chromosome (BAC) tiling path and the number of recombinants determined by cleaved-amplified polymorphic sequence (CAPS) analysis (see Methods). Polymerase chain reaction and DNA gel blot analysis of L*er* and mutant DNAs enabled us to localize the deletions to an area containing three genes (*KNAT1*, a putative xylan endohydrolyase, and a putative inositol 1,3,4-triphosphate 5/6 kinase-like gene).

**(B)** DNA gel blot analysis of genomic DNA from wild-type Columbia (Col) and Landsberg *erecta* (L*er*) and five *bp* mutants probed with a *KNAT1* gene probe. The *KNAT1* gene is deleted in *bp-1*, *bp-2*, *bp-3*, and *bp-5* and has suffered a point mutation in *bp-4* (Table 2). The fainter signal presumably is the result of cross-hybridization with other conserved homeodomain genes and provides a useful loading control.

*BP*::GUS reporter gene construct. Figure 6A shows that the gene is turned on initially at the late globular stage of embryo development in presumptive hypocotyl tissue. Expression persists in the hypocotyl throughout the heart and torpedo stages (Figures 6B and 6C) and into the vegetative stage (data not shown). At later embryonic stages and throughout vegetative development, *BP* is turned on below developing leaf primordia at the shoot apex (Figure 6D). During inflorescence development, *BP* is expressed in pedicels and internodes in cortical tissues (Figures 6E and 6F). During floral development, expression is restricted to the marginal domains of carpels, with no expression in the outer three whorls (Figure 6G). Despite strong expression of *BP* in the hypocotyl and carpels, no obvious defects were observed in these tissues in the *bp* mutant, suggesting that redundant factors compensate for the loss of *BP*.

### Reduced Meristem Function Is Not Evident in *bp*

On the basis of domains of *BP* expression and its role in meristem function, as ascribed in gain-of-function studies (Lincoln et al., 1994; Chuck et al., 1996), we wished to establish whether meristem function is affected in *bp* mutants. We observed no decrease in the number of lateral organs initiated by either the vegetative or inflorescence SAM during *bp* development (data not shown). However, *bp* initiates leaves at a slightly faster rate than does L*er*, and it also flowers slightly earlier (data not shown). This indicates a role for *BP* in the vegetative SAM as a regulator of rates of leaf initiation and floral transition, but not of meristem activity per se.

Recently, Pautot et al. (2001) used a dexamethasone-inducible system to study the effects of ectopic *KNAT2* expression on plant development and found KNAT2 to be sufficient to direct a homeotic conversion of the nucellus of the ovule into a carpel-like structure. The expression of both *BP* and *KNAT2* in placental regions of Arabidopsis gynoecia (Pautot et al. 2001) (Figure 6H) is consistent with a role for class I *KNOX* genes in the regulation of the carpel's ovule-generating meristematic function. To test this hypothesis, we examined *BP* expression in an *ap2* background and found expression at the margin of carpel-like sepals where ovule primordia emerge (Figures 6H and 6I). However, as in the wild-type carpel, *BP* function does not appear to be necessary in *ap2* first-whorl organs for the generation of ovules, because *bp-2 ap2-5* double mutants show an additive phenotype (Figure 6J).

Finally, we examined the genetic relationship between *BP* and *ASYMMETRIC LEAVES2* (*AS2*) during leaf development. *as2* leaves show lobes and the occasional production of ectopic meristems on adaxial surfaces. These phenotypes are consistent with an increase in meristematic identity in the leaf, which is supported by the ectopic expression of *KNOX* genes in *as* leaf tissue (Byrne et al., 2000; Ori et al., 2000; Semiarti et al., 2001). We tested whether *BP* expression in *as2* leaves is necessary for the development of the lobed leaf phenotype by crossing *bp* with *as2*, which is epistatic to *as1* (Ori et al., 2000). Double mutants of *bp-2* and *as2-1* show an additive phenotype (Figure 6K), indicating that *BP* expression is not necessary for the development of the lobed leaf phenotype in *as2* plants.

Collectively, these results indicate that although *BP*'s expression domain and gain-of-function phenotypes implicate a meristematic role (Lincoln et al., 1994; Chuck et al., 1996), redundant factors must compensate for its loss in *bp* plants

**Table 2.** *bp* Mutant Characterization

| Mutant | Origin | Genetic Background | Mutagen[a] | Extent of Deletion[b] |
|---|---|---|---|---|
| *bp-1* | Original *bp* mutant of M. Koornneef | L*er* | EMS | >325 kb |
| *bp-2* | *xt-2* (our nomenclature) | L*er* | FN | >280 kb |
| *bp-3* | *xt-1* (our nomenclature) | L*er* | FN | >365 kb |
| *bp-4* | *bp-m* (gift of M. Metz/N. Ori) | L*er* | EMS | Point mutant |
| *bp-5* | 4265 (gift of A. Sessions) | Columbia | T-DNA | ~150 kb |

[a] EMS, ethyl methanesulfonate; FN, fast neutrons; T-DNA, insertion of T-DNA. In *bp-5*, the T-DNA does not segregate with the mutation.
[b] Deletion end points were mapped by DNA gel blotting and by polymerase chain reaction using primers based on Arabidopsis Genome Initiative sequence information. DNA preparations were shown to be capable of amplification with primers inside and outside the region of the deletions. The absence of a polymerase chain reaction product is scored as a region that is deleted in the mutant.

such that meristem-related processes are not compromised.

## DISCUSSION

Stems of higher plants offer support to the aerial portion of the plant body and serve as conduits for the transport of water and metabolites between roots and leaves. Despite the critical roles played by stems, very little is known about the underlying molecular mechanisms governing their development and morphology. As a first step toward understanding the genetic basis of stem development, we have characterized the *bp* mutant of Arabidopsis, which exhibits bends in inflorescence stems and pedicels as well as reductions in their lengths. Our studies indicate that loss-of-function mutations in both the *BP* and *ERECTA* genes are required to give rise to the *bp* phenotype. These data demonstrate a previously unknown link between *KNOX* gene activity and dicot stem development and raise questions regarding the possible role of meristem-regulating factors during organogenesis.

### The Function of BP and ER during Stem Development

In Arabidopsis, lateral organs are initiated from the peripheral zone of the SAM, requiring the activation of cell division and an alteration in the plane of cytokinesis. Growth is maintained by continued mitosis and cell expansion in both the organ primordia and the intercalary meristem. The anatomy of the stem, however, is very different at nodes and internodes. Discounting heterogeneities in vascular bundle spacing, internodes appear radialized, whereas nodes exhibit asymmetries in vascular bundle patterning and tissue differentiation. Because the aerial parts of plants are initiated repetitively from the SAM, genetic switches must exist to program the two distinct morphologies of the node and internode. Asymmetries that are specified in the peripheral zone during organ initiation and later become manifest at nodes in mature plants must be repressed during internode development so that uniform patterns of tissue differentiation can occur.

In the *bp* mutant, cortical and epidermal tissues of internodes acquire asymmetric patterns of cell differentiation, giving rise to visible stripes of tissue. On the basis of four observations, we propose that these asymmetries are related to the wild-type nodal anatomy. First, Lan nodes exhibit asymmetries in chlorenchyma patterning in lateral regions that appear identical to *bp* stripes in transverse sections. Second, the *erecta* mutation results in reduced density of chlorenchyma distribution below the lateral organs and enhancement of the *bp* stripe phenotype. Third, the wild-type achlorophyllous domains above and around the bases of lateral organs are enhanced in *bp* mutants. Fourth, the *bp* stripe initiates directly beneath the lateral organs, where L*er* chlorenchyma density is reduced, and is linked to the vascular bundle that services the lateral organ. The *bp* internodal stripe, therefore, seems to represent a shift of wild-type nodal asymmetries into internodes, implicating the *BP* and *ER* genes in the regulation of internodal symmetry.

The enhancement of wild-type nodal asymmetries in *bp*, combined with the normal development of chlorenchyma in nonstripe regions, implies that asymmetries in wild-type and mutant stem cortices are caused by the action of a repressor of chlorenchyma development. The influence of this factor may not be confined to chlorenchyma repression, because it also could function to regulate other aspects of nodal differentiation and morphogenesis (e.g., maintenance of active mitosis). The localization of repressor activity adjacent to lateral organs suggests that its function is linked to asymmetries associated with organ initiation in the peripheral zone. We speculate that BP and ER act to restrict the domain of action of the repressor such that in their absence wild-type chlorenchyma asymmetries are enhanced and internode differentiation is altered. An asymmetric increase in the level of such a repressor at the node, next to the lateral organ, may induce sufficient polarity to induce bending in stems.

The link between the *bp* stripe and the vasculature provides evidence that the nodal repressor of chlorenchyma

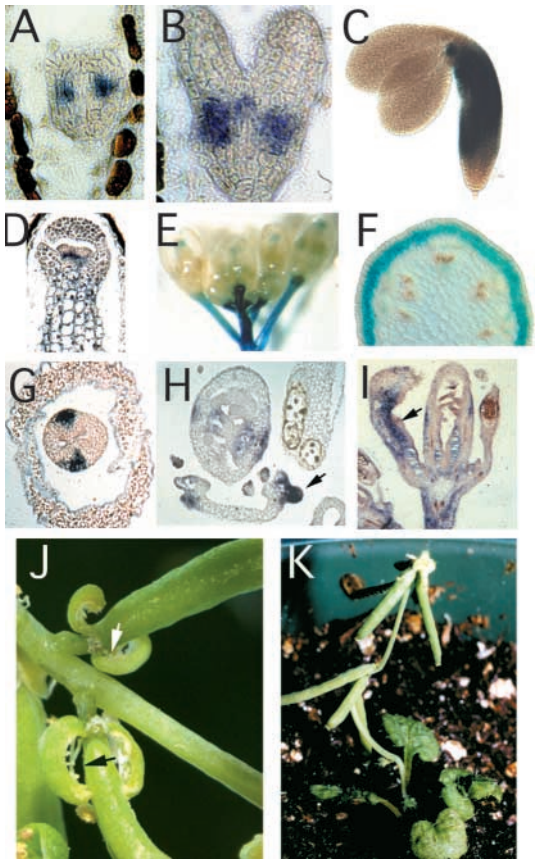


**Figure 6.** Expression of *BP* during Development and in Mutant Backgrounds.

*BP* expression was examined in wild-type plants by both in situ hybridization (**[A]**, **[B]**, **[D]**, **[H]**, and **[I]**) and GUS staining of plants transformed with a *BP*::GUS transgene (**[C]**, **[E]**, **[F]**, and **[G]**).
**(A)** Late globular-stage embryo illustrating expression in cells destined to become the hypocotyl.
**(B)** Late heart-stage embryo. *BP* expression also is observed below the shoot apical meristem.
**(C)** GUS staining of a late torpedo-stage embryo showing intense hypocotyl staining.
**(D)** Longitudinal section of an early torpedo embryo revealing expression at the base of leaf primordia.
**(E)** GUS staining of an inflorescence apex. *BP* is expressed in pedicels, and faint staining can be observed in style cells of the gynoecium.
**(F)** GUS staining of cortical tissue in an internode cross-section.
**(G)** Cross-section through a gynoecium showing GUS staining of marginal tissue.
**(H)** In situ hybridization of *BP* to a cross-section from an *ap2-9* floral bud. In *ap2-9*, *BP* is expressed ectopically in first-whorl carpel-like sepals (arrow).
**(I)** In situ hybridization with an *ap2-2* plant revealing ectopic staining of sepals (arrow).
**(J)** Floral phenotype of a *bp-2 ap2-5* double mutant. Arrows point to ovules arising on the margins of the sepals.
**(K)** Unaltered *as2* leaf morphology in a *bp-2 as2-1* double mutant.

development is related to the vasculature. Our data are consistent with the flux of repressor basipetally from the node through the vasculature to alter differentiation in overlying tissue layers. However, we cannot exclude the possibility that the repressor has independent functions in both positioning vascular bundles and effecting cortical and epidermal differentiation in internodes. The action of the repressor in *bp* stems reveals that mutant internodes develop as mosaics, with individual sectors represented by a vascular bundle and overlying cortex and epidermis. At a given transection along an internode, units differ in the concentration of repressor with which they are or have been associated. In the wild type, therefore, repression of the action of this "asymmetrizing" molecule by BP and ER leads indirectly to a normalization of unit identities in internodes, which underlies the switch between asymmetric nodal organization and radialized internodes. Supporting evidence for a link between the *bp* stripe and the vasculature comes from other studies examining *KNOX* gene function. For example, in the maize *knotted1* mutant, leaf blade cells over veins differentiate into sheath-like cells as a result of the misexpression of *KNOTTED1* (Smith et al., 1992), and overexpression of *BP* in Arabidopsis leads to ectopic meristem formation near veins (Chuck et al., 1996).

### Pedicel Dorsoventrality Is Specified by *BP*

Achlorophyllous stripes also are evident in pedicels of *bp*, although they occur only in abaxial regions. The similarity of abaxial *bp* pedicel histology to that of stripes in internodes indicates that BP and ER also are required to restrict the action of a chlorenchyma repressor in pedicels. The genes' dispensability in adaxial pedicel domains reveals that Arabidopsis pedicels exhibit a heretofore unrecognized dorsoventral polarity. Asymmetry in the adaxial-abaxial plane is evident in leaves and floral organs of most higher plants and recently has been examined at the genetic level (for review, see Bowman, 2000), but it has not been reported in stem tissue. There are two potential sources of asymmetries that could direct pedicel dorsoventrality.

The first of these is radial polarities inherent to the inflorescence axis. Recently, the relative proximity of primordial adaxial and abaxial leaf domains to the center of the shoot axis was suggested to underlie the development of leaf dorsoventrality (McConnell et al., 2001). This model is based on the identity, expression patterns, and mutant phenotypes of the Arabidopsis *PHB* and *PHV* genes, members of the HD-ZIP class of putative ligand binding transcription factors. These authors propose that PHB translates radial asymmetries in the shoot to dorsoventral leaf identities by perceiving SAM-derived positional information in dorsal leaf domains and activating an adaxial-specific developmental program. Similar mechanisms also may act in pedicel tissue, culminating in the acquisition of dorsoventral polarity. In wild-type plants, dorsoventral pedicel asymmetries are masked by the

action of BP and ER but become evident in *bp* plants having adaxial chlorenchyma only. In this situation, redundant factors would function to restrict the activity of the chlorenchyma repressor to abaxial pedicel domains, and BP and ER would "adaxialize" the pedicel so that dorsoventral asymmetries do not develop.

The second mechanism underpinning dorsoventral pedicel asymmetries in *bp* may relate to asymmetry in pedicel vasculature patterning. We have observed that adaxial vascular bundles usually are much smaller and less distinct than those in abaxial regions. This property probably is related to the branching of vasculature into lateral organs from positions below the node. If the chlorenchyma repressor acts in a vasculature-dependent manner in pedicels as well as internodes, then dorsoventral vasculature patterning asymmetries could underlie adaxial–abaxial differences in *bp* pedicel histologies. In either situation, it appears that the concentration of repressor action on the abaxial sides of pedicels induces sufficient polarity for downward bends to develop in the *bp* mutant. It is unclear how the receptor kinase encoded by *ERECTA*, and a putative transcription factor encoded by *BP*, are engaged in regulating stem architecture. To identify the molecules involved in this pathway(s), we are now using microarray analyses to identify other genes regulated by *BP* and are characterizing suppressor mutants of *bp* in which its defects are ameliorated.

### BP and Meristem Function

Numerous studies have implicated *KNOX* genes as regulators of meristem function. Arabidopsis plants homozygous for strong *stm* mutations fail to develop the apical cellular organization characteristic of active SAMs and as a result only rarely produce aerial organs postgerminatively (Barton and Poethig, 1993). Recessive mutations in the maize *KNOTTED1* gene lead to a reduction in inflorescence branching and a loss of shoot meristem function (Kerstetter et al., 1997; Vollbrecht et al., 2000). Similarly, overexpression of *KNOX* genes in maize, tobacco, rice, and Arabidopsis leads to morphogenetic abnormalities that are consistent with a role for these genes during meristem development. Localized cell proliferation in "knots" of maize leaves ectopically expressing KNOTTED1 can be interpreted as a regional increase in meristematic identity. In tobacco, *KNOX* overexpression induces the formation of meristems on leaves (Nishimura et al., 2000), and in Arabidopsis, the ectopic formation of SAMs on the adaxial surfaces of 35S::*BP* vegetative and inflorescence leaves indicates that BP is sufficient to initiate meristem development. Thus, in certain situations, BP can activate meristem function, but redundant factors must substitute for it in *bp* meristematic tissue. Such factors could include the closely related class I *KNOX* genes *STM*, *KNAT2*, and *KNAT6* (Lincoln et al., 1994; Semiarti et al., 2001). The identification of null mutants for other class I *KNOX* genes will help establish the mechanisms underlying this redundancy.

During evolution, meristem-associated factors such as BP may have acquired a role in controlling the development of nonmeristematic tissues such as internodes. Notably, loss-of-function mutations in the rice class I *KNOX* gene *OSH15* also give rise to defects during stem development (Sato et al., 1999). *osh15* internodes are shorter, and hypodermal sclerenchymatous cells fail to differentiate. By cladistic analyses, *OSH15* is the rice ortholog of both *BP* and *RS1* of maize (data not shown). The close sequence similarity of *BP* and *OSH15*, combined with their involvement in similar developmental processes, suggests that the *BP*/*OSH15* ancestor gene may have acquired a role in stem development before the divergence of dicots and monocots.

## METHODS

### Plant and Genetic Materials

Seed of *Arabidopsis thaliana*, ecotype Landsberg *erecta* (L*er*), were used for most experiments reported. Fast neutron–mutated L*er* M2 seed were purchased from Lehle Seeds (Round Rock, TX). Seed of the mapping mutant *brevipedicellus* (*bp*), Landsberg seed wild type for the *ERECTA* gene (Lan), bacterial artificial chromosome clones, *ap2-5* mutant seed, and *as2-1* mutant seed were obtained from ABRC (Ohio State University, Columbus). Plants were grown indoors under constant illumination with fluorescent bulbs. Additional mutant lines were provided by Drs. Camille Steber (Washington State University, Pullman), Allen Sessions (University of California, San Diego), Matt Metz (University of California, Berkeley), and Naomi Ori (Plant Gene Expression Center, Albany, CA). The *BP*::β-glucuronidase (GUS) transgenic line was provided by Sarah Hake and described by Ori et al. (2000). Crosses between *bp-2* and *ap2-5* and between *bp-2* and *as2-1* were generated and confirmed as double mutants by morphological criteria.

### Mapping of the *bp* Mutation and Mutant Rescue

Complementation tests demonstrated that the *bp* mutants are allelic. For subsequent genetic analyses, *bp-2* was used and was backcrossed twice into L*er* plants. To establish a mapping population, *bp-2* plants were crossed with Columbia and the progeny were selfed. DNA was isolated from F2 plants exhibiting a *bp* phenotype and was used for both simple sequence length polymorphism and restriction fragment length polymorphism analyses. DNA from plants recombinant for either the nga8 or nga12 simple sequence length polymorphism locus then was used for additional mapping by developing cleaved-amplified polymorphic sequence markers (Konieczny and Ausubel, 1993; see http://www.arabidopsis.org/servlets/TairObject?id=115andtype=marker for details of primers and cleaved-amplified polymorphic sequence data).

Molecular mapping and subsequent DNA gel blot analyses suggested that the *KNAT1* gene may be responsible for the *bp* phenotype. We amplified a 4.7-kb fragment from genomic DNA using the primers 5′-GGACTAGTTTCGGTCTAGTGCAGTGATGAGG-3′ and 5′-TGGTCGACTGTCCGCATCAGATGACGAGTG-3′. This strategy introduced SpeI and SalI sites at the ends, and after SpeI–SalI digestion, the fragment was mobilized into pGVPT-HPT (Becker et al.,

1992). The binary construct was introduced into *Agrobacterium tumefaciens* strain GV3101, and *bp* mutants were transformed and selected by the dipping protocol described by Clough and Bent (1998).

### Tissue Preparation for Light Microscopy/Cell Length Measurements

Internode segments of ~5 mm were placed in Jeffrey's solution (10% aqueous nitric acid and 10% aqueous chromic acid [1:1]) for 4 or more hr at room temperature until the epidermis began to separate. Segments of epidermis with the attached outermost cell layer of cortical parenchyma were collected and washed in several changes of water. For cell length measurements, tissue was mounted in chloral hydrate:glycerol:water (8:2:1) and observed by Nomarski interference microscopy. For photomicrography, epidermal tissue was stained overnight in 1% aqueous safranin, dehydrated quickly in a graded ethanol series followed by 100% ethanol:xylene (1:1) and pure xylene changes, and mounted in Permount (Fisher Scientific, Nepean, Ontario).

To examine the morphology of tissue sections, 2-mm tissue segments were fixed in cold FAA (50 mL of 95% ethanol, 5 mL of glacial acetic acid, 10 mL of 37% formaldehyde, and 35 mL of distilled water) for a minimum of 48 hr and stored in FAA at 4°C. Tissue was washed in 70% ethanol and double distilled water before secondary fixation in 1% aqueous osmium tetroxide at room temperature for 2 hr. After distilled water washes, tissue was dehydrated in an acetone series and infiltrated and embedded in Spurr's low-viscosity resin. Sections (1.5 μm thick) were cut using glass knives and an ultramicrotome. Sections were stained with 0.05% toluidine blue in 0.05% aqueous borax and mounted in Cytoseal 60 (Stephens Scientific, Riverdale, NJ). Images were captured with a Zeiss (Jena, Germany) Axiophot photomicroscope.

### Scanning Electron Microscopy

Segments of internode, inflorescence axis, and pedicels were fixed and stored in cold 70% FAA as described above. Tissue was washed in 70% ethanol and dehydrated in a graded ethanol series, critical point dried, mounted and gold coated on aluminum stubs, and viewed with an Hitachi (Tokyo, Japan) scanning electron microscope at 20 or 25 kV.

### Hand Sectioning of Stems and Pedicels

Mature plants were placed under tap water, and a razor blade was used to generate thin sections of live material. Sections were collected with a Pasteur pipette and mounted in 50% glycerol for microscopy.

### In Situ Hybridization and GUS Histochemical Assays

In situ hybridization was performed as described by Jackson et al. (1994). Sense and antisense probes used for *BP* (*KNAT1*) were as described by Lincoln et al. (1994). GUS histochemical assays were performed as described by Ori et al. (2000).

## ACKNOWLEDGMENTS

The authors thank Sarah Hake, Rob Martienssen, Mary Byrne, Matt Metz, and Camille Steber for sharing materials and information. We also are indebted to John Tang, Raymond Orr, Barbara Ambrose, Bob Schmidt, Marty Yanofsky, Medard Ng, Dino Balkos, and Thomas Berleth for assistance with techniques and their advice about this project. We appreciate the helpful comments of two anonymous reviewers. We acknowledge ABRC for providing seed and bacterial artificial chromosome clones and Nancy Dengler and Clare Hasenkampf for sharing equipment and for valuable comments on the manuscript. We thank Annette Rzepczyk for excellent technical assistance. S.J.D. was supported by a postgraduate fellowship from the Natural Sciences and Engineering Research Council of Canada (NSERC) and a traveling fellowship from The Company of Biologists, Ltd. G.C. was supported by a University of California fellowship (to Sarah Hake). This research was supported by a grant from NSERC to C.D.R.

Received September 6, 2001; accepted November 16, 2001.

## REFERENCES

**Arabidopsis Genome Initiative** (2000). Analysis of the genome sequence of the flowering plant *Arabidopsis thaliana*. Nature **408,** 796–815.

**Barton, M.K., and Poethig, R.S. (1993).** Formation of the shoot apical meristem in *Arabidopsis thaliana*: An analysis of development in the wild type and in the *shoot meristemless* mutant. Development 119, 823–831.

**Becker, D., Kemper, E., Schell, J., and Masterson, R.** (1992). New plant binary vectors with selectable markers located proximal to the left T-DNA border. Plant Mol. Biol. **20,** 1195–1197.

**Bowman, J.L.** (2000). Axial patterning in leaves and other lateral organs. Curr. Opin. Genet. Dev. **10,** 399–404.

**Byrne, M.E., Barley, R., Curtis, M., Arroyo, J.M., Dunham, M., Hudson, A., and Martienssen, R.A.** (2000). *asymmetric leaves 1* mediates leaf patterning and stem cell function in Arabidopsis. Nature **408,** 967–971.

**Chuck, G., Lincoln, C., and Hake, S.** (1996). KNAT1 induces lobed leaves with ectopic meristems when overexpressed in Arabidopsis. Plant Cell **8,** 1277–1289.

**Clough, S.J., and Bent, A.F.** (1998). Floral dip: A simplified method for *Agrobacterium*-mediated transformation of *Arabidopsis thaliana*. Plant J. **16,** 735–743.

**Hanzawa, Y., Takahashi, T., and Komeda, Y.** (1997). *ACL5*: An Arabidopsis gene required for internodal elongation after flowering. Plant J. **12,** 863–874.

**Jackson, D., Veit, B., and Hake, S.** (1994). Expression of maize *KNOTTED1* related homeobox genes in the shoot apical meristem predicts patterns of morphogenesis in the vegetative shoot. Development **120,** 405–413.

**Kerstetter, R., Vollbrecht, E., Lowe, B., Veit, B., Yamaguchi, J., and Hake, S.** (1994). Sequence analysis and expression patterns divide the maize *KNOTTED 1*-like homeobox genes into 2 classes. Plant Cell **6,** 1877–1887.

**Kerstetter, R.A., Laudencia-Chingcuanco, D., Smith, L.G., and Hake, S.** (1997). Loss-of-function mutations in the maize homeobox gene, *knotted1*, are defective in shoot meristem maintenance. Development **124,** 3045–3054.

**Kerstetter, R.A., Bollman, K., Taylor, R.A., Bomblies, K., and Poethig, R.S.** (2001). KANADI regulates organ polarity in Arabidopsis. Nature **411,** 706–709.

**Konieczny, A., and Ausubel, F.M.** (1993). A procedure for mapping Arabidopsis mutations using codominant ecotype-specific PCR-based markers. Plant J. **4,** 403–410.

**Koornneef, M., van Eden, J., Hanhart, C.J., Stem, P., Braaksma, F.J., and Feenstra, W.J.** (1983). Linkage map of *Arabidopsis thaliana*. J. Hered. **74,** 265–272.

**Lincoln, C., Long, J., Yamaguchi, J., Serikawa, K., and Hake, S.** (1994). A *knotted 1*-like homeobox gene in *Arabidopsis* is expressed in the vegetative meristem and dramatically alters leaf morphology when overexpressed in transgenic plants. Plant Cell **6,** 1859–1876.

**Long, J.A., Moan, E.I., Medford, J.I., and Barton, M.K.** (1996). A member of the KNOTTED class of homeodomain proteins encoded by the *STM* gene of Arabidopsis. Nature **379,** 66–69.

**McConnell, J.R., Emery, J., Eshed, Y., Bao, N., Bowman, J., and Barton, M.K.** (2001). Role of PHABULOSA and PHAVOLUTA in determining radial patterning in shoots. Nature **411,** 709–713.

**McCourt, P.** (1999). Genetic analysis of hormone signaling. Annu. Rev. Plant Physiol. Plant Mol. Biol. **50,** 219–243.

**Muehlbauer, G.J., Fowler, J.E., Girard, L., Tyers, R., Harper, L., and Freeling, M.** (1999). Ectopic expression of the maize homeobox gene *Liguleless3* alters cell fates in the leaf. Plant Physiol. **119,** 651–662.

**Ng, M., and Yanofsky, M.F.** (2001). Function and evolution of the plant MADS-box gene family. Nat. Rev. Genet. **2,** 186–195.

**Nishimura, A., Tamaoki, M., Sakamoto, T., and Matsuoka, M.** (2000). Over-expression of tobacco *knotted*1-type class 1 homeobox genes alters various leaf morphology. Plant Cell Physiol. **41,** 583–590.

**Ori, N., Eshed, Y., Chuck, G., Bowman, J., and Hake, S.** (2000). Mechanisms that control knox gene expression in the *Arabidopsis* shoot. Development **127,** 5523–5532.

**Pautot, V., Dockx, J., Hamant, O., Kronenberger, J., Grandjean, O., Jublot, D., and Traas, J.** (2001). KNAT2: Evidence for a link between knotted-like genes and carpel development. Plant Cell **13,** 1719–1734.

**Reiser, L., Sanchez-Baracaldo, P., and Hake, S.** (2000). Knots in the family tree: Evolutionary relationships and functions of knox homeobox genes. Plant Mol. Biol. **42,** 151–166.

**Sato, Y., Sentoku, N., Miura, Y., Hirochika, H., Kitano, H., and Matsuoka, M.** (1999). Loss-of-function mutations in the rice homeobox gene *OSH15* affect the architecture of internodes resulting in dwarf plants. EMBO J. **18,** 992–1002.

**Schneeberger, R.G., Becraft, P.W., Hake, S., and Freeling, M.** (1995). Ectopic expression of the knox homeobox gene *ROUGH SHEATH1* alters cell fate in the maize leaf. Genes Dev. **9,** 2292–2304.

**Semiarti, E., Ueno, Y., Tsukaya, H., Iwakawa, H., Machida, C., and Machida, Y.** (2001). The *asymmetric leaves2* gene of *Arabidopsis thaliana* regulates formation of a symmetric lamina, establishment of venation and repression of meristem-related homeobox genes in leaves. Development **128,** 1771–1783.

**Sentoku, N., Sato, Y., and Matsuoka, M.** (2000). Overexpression of rice *OSH* genes induces ectopic shoots on leaf sheaths of transgenic rice plants. Dev. Biol. **220,** 358–364.

**Sinha, N.R., Williams, R.E., and Hake, S.** (1993). Overexpression of the maize homeobox gene, *KNOTTED-1*, causes a switch from determinate to indeterminate cell fates. Genes Dev. **7,** 787–795.

**Smith, L.G., Greene, B., Veit, B., and Hake, S.** (1992). A dominant mutation in the maize homeobox gene, *Knotted-1*, causes its ectopic expression in leaf cells with altered fates. Development **116,** 21–30.

**Torii, K.U., Mitsukawa, N., Oosumi, T., Matsuura, Y., Yokoyama, R., Whittier, R.F., and Komeda, Y.** (1996). The Arabidopsis *ERECTA* gene encodes a putative receptor protein kinase with extracellular leucine-rich repeats. Plant Cell **8,** 735–746.

**Tsukaya, H., Naito, S., Redei, G.P., and Komeda, Y.** (1993). A new class of mutations in *Arabidopsis thaliana*, *ACAULIS1*, affecting the development of both inflorescences and leaves. Development **118,** 751–764.

**Vollbrecht, E., Reiser, L., and Hake, S.** (2000). Shoot meristem size is dependent on inbred background and presence of the maize homeobox gene, knotted1. Development **127,** 3161–3172.

**Williams-Carrier, R.E., Lie, Y.S., Hake, S., and Lemaux, P.G.** (1997). Ectopic expression of the maize *kn1* gene phenocopies the *Hooded* mutant of barley. Development **124,** 3737–3745.

**Yokoyama, R., Takahashi, T., Kato, A., Torii, K.U., and Komeda, Y.** (1998). The *Arabidopsis ERECTA* gene is expressed in the shoot apical meristem and organ primordia. Plant J. **15,** 301–310.